Geophysical Research Letters

RESEARCH LETTER
10.1029/2019GL086640

The Role of Seismic and Slow Slip Events in Triggering the 2018 *M*7.1 Anchorage Earthquake in the Southcentral Alaska Subduction Zone

M. Segou[1] **and T. Parsons**[2]

[1]The Lyell Centre, British Geological Survey, Edinburgh, UK, [2]U.S. Geological Survey, Menlo Park, CA, USA

Key Points:
- Stress effects from the 1964 postseismic source and a long-lasting slow slip event promoted the recent 2018 Anchorage event
- The slow slip events occur in the 1964 stress shadow, farther downdip of the 1964 coseismic slip distributions but within the upper limit of its afterslip
- The slow slip events modulate the deeper shallow depth low magnitude seismicity and capture the post-1964 triggered seismicity

Supporting Information:
- Supporting Information S1

Correspondence to:
M. Segou,
msegou@bgs.ac.uk

Citation:
Segou, M., & Parsons, T. (2020). The role of seismic and slow slip events in triggering the 2018 *M*7.1 Anchorage earthquake in the Southcentral Alaska subduction zone. *Geophysical Research Letters*, *47*, e2019GL086640. https://doi.org/10.1029/2019GL086640

Received 13 DEC 2019
Accepted 18 APR 2020
Accepted article online 23 APR 2020

Abstract The *M*7.1 2018 Anchorage earthquake occurred in the bending part of the subducting North Pacific plate near the geometrical barrier formed by the underthrusting Yakutat terrane. We calculate the triggering potential related with stress redistribution from deformation sources including the *M*9.2 1964 earthquake coseismic slip, postseismic deformation, slip from regional $M > 5$ earthquakes, and the cumulative slip of previously detected slow slip events over the past 55 years. We investigate the deeper shallow depth (20–60 km) seismicity response to these perturbations using an epidemic type aftershock sequence model to describe earthquake-to-earthquake interactions. The statistical forecast captures the triggered seismicity during the 1983 *M*6+ aftershocks in Columbia Bay but performs poorly during the slow slip event period between 1992.0 and 2004.8 that presents a statistically significant rate change (β, $Z > 2$; $M < 4.0$). We find that stress effects from the 1964 postseismic source and the 12-year-long slow slip event (~*M*7.8) contribute to the 2018 Anchorage earthquake occurrence and that slow slip events modulate the deeper shallow depth seismicity patterns in the region.

Plain Language Summary The 2018 *M*7.1 Anchorage earthquake happened within a bending part of the downgoing slab beneath Southcentral Alaska. The earthquake was encouraged by stress accumulation caused by slow slip on the interface between the slab and the North American plate. Slow slip events also more than doubled the $M \geq 3$ earthquake rate in the Cook Inlet beginning in the 1990s.

1. Introduction

Large magnitude ($M > 8.0$) earthquakes in subduction zones are most commonly megathrust ruptures that are associated with multiple hazard phenomena such as severe ground shaking, tsunamis, and landslides. However, intraslab earthquakes, such as the 2018 *M*7.1 Anchorage (Ruppert & Witter, 2019), the 2017 *M*7.1 Puebla (Alberto et al., 2018), and the 1999 Oaxaca (Singh et al., 2000) in Mexico among others, are associated with extended structural damage and loss of life, highlighting their contribution to seismic hazard (Choy & Kirby, 2004). It is difficult to identify intraslab faults before they rupture, and their often undetermined recurrence intervals make them particularly difficult to account for in time-dependent seismic hazard assessments. Therefore, understanding mechanical interactions between intraslab and interslab earthquakes, and their triggering mechanisms is necessary to identify high-hazard locations and periods (e.g., Lin & Stein, 2004).

Earthquakes can be triggered by the passage of seismic waves (dynamic triggering) (e.g., Hill & Prejean, 2015, and references therein) and/or distortion of the crust caused by coseismic slip on faults (static triggering) (e.g., Harris, 1998, and references therein), with effects persisting from days to years following a large mainshock (e.g., Omori, 1894; Parsons, 2002). Until recently, only past earthquakes were considered as triggering sources, but the advance of geodetic networks reveals that aseismic deformation on the plate boundary fault can equal, if not exceed, the cumulative moment release of subduction earthquakes (Kano et al., 2019; Kobayashi & Tsuyuki, 2019; Voss et al., 2017).

Dmowska and Lovison (1988) and (Lin and Stein (2004) demonstrated a general case for increased failure stress caused by interactions between interplate and normal intraslab earthquakes. Mikumo et al. (2002) analyzed the link between the *M*7.8 1978 to *M*7.5 1999 Oaxaca and the *M*8.1 1985 to *M*7.1 1997 Michoacan earthquake pairs and suggested that the intermediate-depth normal events occur as a mechanical consequence following "large thrust earthquakes with low-dip angles and shallow depths." Lay et al. (2017) give examples of coseismic and delayed triggering in the 2006–2009 Central Kuriles, 2009

Samoa/Tonga, and 2011–2012 Japan trenches. Choy and Kirby (2004) suggested that the spatial and temporal connection between large magnitude interface-intraslab pairs in the 1997 Chile, 2001 El Salvador, and 1999–2000 Kodiak sequences, supporting various coupling modes between deeper normal and shallow ($h < 70$ km; Choy & Kirby, 2004) thrust earthquakes. Wallace et al. (2014) suggested that the intraslab 2014 *M*6.4 Eketahuna earthquake in New Zealand was triggered by the 2013 Kapiti slow slip event, and Segou and Parsons (2018) supported that incorporation of aseismic phenomena, such as afterslip, was influential in triggering the deep, normal-fault *M*7.1 Puebla earthquake in Mexico.

Understanding the frequency and the triggering processes behind the occurrence of intraslab events is critical for seismic hazard since their often increased apparent stress and radiated energy can be the underlying cause of extended damage for populations located just above the bend of the subducting plate (Bilek & Lay, 2018; Choy & Kirby, 2004). Slow slip events are known to trigger small magnitude seismicity in swarms (Ozawa et al., 2003), low-frequency events that invade the locked megathrust zone through stress transfer (Kano et al., 2019), and small repeating events with slow slip involvement (Kato et al., 2012). In recent years, the precursory role of slow slip events in the nucleation processes of large shallow megathrust earthquakes has been revealed in locations with dense geodetic networks, such as in Costa Rica (Voss et al., 2018), Japan (Ito et al., 2013; Kato et al., 2012), Chile (Ruiz et al., 2014), and Mexico (Maury et al., 2018). In this study we focus on the contributions of past large earthquakes and long-duration slow slip events to investigate seismicity patterns and the triggering processes that culminated in the 2018 Anchorage intraslab earthquake.

2. Seismicity and Stress Changes

In Southcentral Alaska, the geodynamic setting is dominated by active subduction of the Pacific plate under the North American plate with velocites reaching 43–47 mm yr^{-1} (DeMets et al., 2010) where the *M*9.2 1964 Great Alaska earthquake occurred. The 2018 *M*7.1 Anchorage earthquake produced the strongest post-1964 shaking in the city, causing structural damage related to strong ground motion and extended liquefaction phenomena (Randall et al., 2019). Expanded geodetic networks have led to the observation of long-lasting slow slip events in Cook Inlet (Li et al., 2016; Ohta et al., 2006). The first slow slip event lasted 12 years between 1992.0 and 2004.8 (Slow Slip Event 1; moment equivalent to ~*M*7.8), and the later slow slip event lasted 2 years between 2009.85 and 2011.81 (Slow Slip Event 2; moment equivalent to ~*M*7.2) (Li et al., 2016).

The locations of the slow slip events are within the middle section of the downdip extension of the post-1964 afterslip distributions that dominate the 30-year cumulative displacements (Li et al., 2016) extending the previous work of these coauthors from Suito and Freymueller (2009) regarding deformation sources in the area.

We investigate the influence of the 1964 Great Alaska earthquake and the role of the subsequent slow slip events in triggering the 2018 *M*7.1 Anchorage event. We describe the physical interaction between earthquakes and slow slip events using the Coulomb failure stress estimate (CF) given by the equation,

$$CF = \left|\overline{\tau_f}\right| + \mu'(\sigma_n),\ \mu' = \mu(1 - B_k) \tag{1}$$

where $\left|\overline{\tau_f}\right|$ is the change in shear stress (fault parallel) on the receiver fault, μ' is the apparent coefficient of friction ($0 \leq \mu' \leq 0.8$), σ_n is the change in normal stress, and B_k is Skempton's coefficient, which accounts for pore fluid pressure (Rice, 1992). Stress values are estimated by slipping an elastic dislocation representation for each source model using Okada's (1992) equations.

We calculate the expected stress changes on the 2018 Anchorage rupture plane using the 1964 coseismic rupture model of Ichinose et al. (2007) that combined seismic, tsunami, and geodetic data, the postseismic model of Suito and Freymueller (2009), and the cumulative slip for the slow slip events determined by Li et al. (2016). The geometry of the Alaskan megathrust is taken from the U.S. Geological Survey (USGS) SLAB 2.0 subduction model (Hayes, 2018). The 2018 Anchorage plane representation is taken from the finite fault model of the USGS-National Earthquake Information Center (NEIC), available from the National Earthquake Information Center event page (source: https://earthquake.usgs.gov/earthquakes/eventpage/ak20419010/executive) and the recent Liu et al. (2019) results. The USGS-NEIC determined the 30 November 2018 (17:29:29 UTC) event at hypocenter 46.7 km depth, at 61.346°N, 149.955°W with the finite fault model favoring an east dipping plane with strike 16° and dip 29°, whereas Liu et al. (2019)

reported a best fit solution supporting a west dipping plane with strike 186° and dip 65° with a deeper hypocenter at 55 km.

In Figure 2a the Anchorage earthquake rupture plane is represented by the USGS-NEIC finite fault model, we find that the estimated average coseismic stress changes of the 1964 earthquake at the hypocenter (Figure 2; mean value represented by point with error bars showing the standard deviation) are miniscule, -0.06 ± 0.09 MPa, similar to the stress changes value related with Slow Slip Event 2, -0.03 ± 0.02 MPa. Clearly, the 1964 postseismic effects and the long duration Slow Slip Event 1 are more significant, reaching 0.26 and 0.13 MPa at the 2018 hypocenter, respectively. Then, we estimate further the stress values on the nonzero slip location of the fault plane from the above deformation sources. We find that the average stress value (Figure 2; horizontal lines with shaded area representing the standard deviation) on the 2018 Anchorage plane is 0.05 (±1.14), 0.13 (±1.24), 0.26 (±0.41), and 0.09 (±0.24) MPa for the 1964 coseismic, postseismic, Slow Slip Event 1, and Slow Slip Event 2 sources, respectively.

In Figure 2b the Anchorage earthquake rupture plane is represented by the Liu et al. (2019) solution that shows a high-angle west dipping plane and a deeper hypocentral depth. We find that the estimated 1964 coseismic and postseismic stress changes at the 2018 hypocenter are 0.10 (±0.09) and 0.21 (±0.10) MPa, respectively, while the stress contribution from slow slip events is less: −0.0087 (±0.02) and − 0.019 (±0.001) MPa. We find that the average stress value on the Liu et al. (2019) solution of the 2018 Anchorage plane is −0.28 (±0.5), 0.59 (±0.9), 0.16 (±0.99), and −0.05 (±0.06) MPa for the 1964 coseismic, postseismic, Slow Slip Event 1, and Slow Slip Event 2 sources, respectively. Thus both 2018 Anchorage rupture plane solutions show stress increases from 1964 postseismic effects and slow slip events to varying degrees.

We consider the 2008–2013 transient deformation event (Rousset et al., 2018) although it overlaps with the Slow Slip Event 2 period, and its maximum slip area is within the north patch of Slow Slip Event 2. We find that the maximum stress changes using the 2008–2013 transient deformation source is 3.13 and 0.27 kPa using as receiver plane the USGS-NEIC and the Liu et al. (2019) finite fault solution, respectively.

We also investigate the role of slow slip events in triggering the deeper shallow (20–60 km) depth seismicity in general; the spatial extent of the data used is shown in Figure 1. Investigating the seismicity response to aseismic transients through statistical modeling based on epidemic type aftershock sequence (ETAS) model is a robust method that extends even into inversion techniques for determining the past occurrence of those transients in the absence of geodetic measurements (Llenos & McGuire, 2011). Our effort here is to model the earthquake-to-earthquake interactions through the ETAS model and to evaluate the stress effects from large regional earthquakes so that we can track the unique effect of the slow slip transients to the target seismicity. To isolate the effects of aftershocks from large regional earthquakes, we describe the expected seismicity resulting from earthquake-to-earthquake interaction using an ETAS model (Ogata, 1985) fit to the Omori decay using the function:

$$\lambda(t) = \mu + \sum_{i:\, t_i < t} K_0 e^{\alpha(M - M_{\text{cut}})} \cdot c^{p-1} (t + c)^{-p} (p - 1)) \; \# \tag{2}$$

where μ is the background rate, which is a time-independent, and spatially heterogeneous Poisson process. The summation term represents the triggering effects from all preceding earthquakes occurring at $t_i < t$. The parameter K regulates the short-term aftershock productivity by a parent event with magnitude M equal or above a minimum triggering magnitude; α establishes the efficiency of earthquakes in triggering aftershocks as a function of magnitude.

We used the NEIC earthquake catalog in the Cook Inlet region to assess whether any seismicity patterns occurred within the period of the slow slip events that could not be explained by earthquake-to-earthquake interaction mechanisms. We consider deeper shallow depth earthquakes (20–60 km) to avoid shallow seismicity on active faults in the area, provided as supplementary material. Our primary target in the ETAS model is the long-term aftershock decay following the M9.2 1964 Great Alaska earthquake. We use the pre-1990 seismicity (Ruppert & West, 2019) to model the long-term decay. Due to the sparse seismic networks in the 1960s to 1970s, we determine the p value = 1.27, and $\alpha = 3.0$ by using higher magnitude ($M \geq 5.0$) events from the first 6 months after the 1964 earthquake and extrapolate

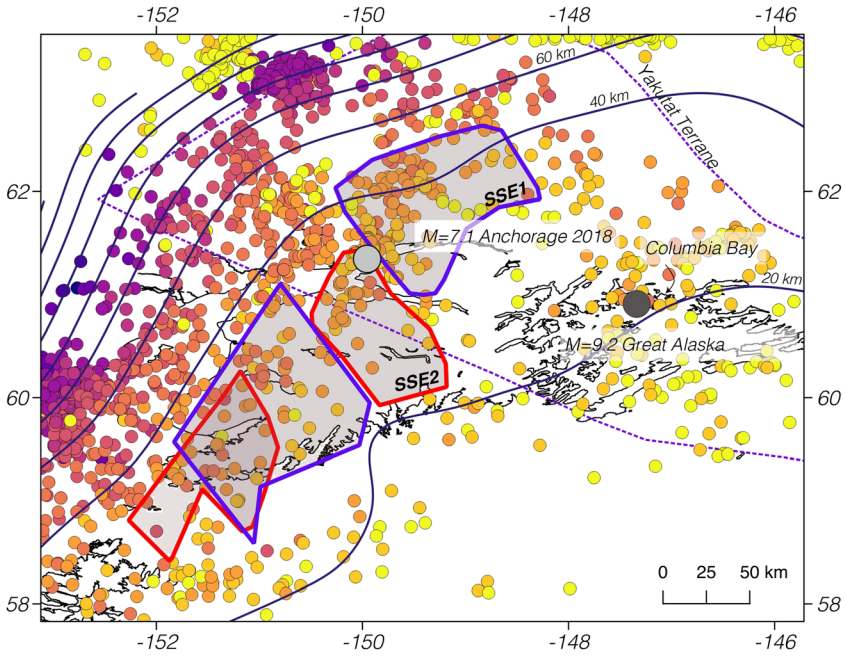

Figure 1. Seismic and aseismic events in the Southcentral Alaska subduction zone between the 1964 *M*9.2 Great Alaska (black circle) and the 2018 *M*7.1 Anchorage (gray circle) earthquakes. The $M \geq 4$ earthquakes color coded with depth (0–20 km; yellow; 20–40 km light orange; 40–60 km; dark orange; 60–80 km magenta; 80–100 km dark magenta; >100 km blue) overlay the spatial patterns of the slow slip events with Slow Slip Event 1: 1992.0–2004.8 (~*M*7.8) (blue bold lines, Slow Slip Event 1 main patches), Slow Slip Event 2: 2009.85–2011.81 (~*M*7.2) (red bold lines, Slow Slip Event 2 main patches) (Li et al., 2016). The geometry of the megathrust is taken from the SLAB2.0 Alaska subduction model (Hayes, 2018) and the boundaries of the Yukutat terrane from Eberhart-Phillips et al. (2006).

assuming a b value = 1. We then fix the p value, and we take $c = 0.018$, $K = 0.21$ from a past statistical model for Alaska (Wei et al., 2012).

The resulting ETAS model accurately captures the peak in triggered seismicity related with the July 1983 *M*6.4 and September 1983 *M*6.3 Columbia Bay earthquakes (Figure 3). The middle to late 1983 aftershocks are described adequately by the statistical models providing an excellent benchmark time period for validating the ETAS parameterization using frequently employed log-likelihood statistics. The modified number (N) test (Zechar et al., 2010) provides a robust evaluation for the effectiveness of the statistical earthquake-to-earthquake interaction model with the metrics within the July–September aftershock period equal to $\delta_1 = 0.001, 0.0579, 0.0997$ and $\delta_2 = 0.9995, 0.9769, 0.9334$ corresponding to nonrejection for August–September 1983 with an underestimation in July, which is often observed in early time periods for ETAS affected by early aftershock incompleteness (Segou et al., 2013). We therefore conclude that the ETAS model is also an accurate statistical descriptor of earthquake-to-earthquake interaction for the pre–slow slip event period (1990–1992). In the pre–slow slip event period, the average expected monthly rate of ~1–2 $M \geq 3.0$ events is consistent with the post-1964 decay predicted by the ETAS model with a few spikes related to aftershocks from low magnitude events. Although the moment rate function of the Slow Slip Event 1 is not available (1992–2004; Figure 3 in magenta), we observe that the shape of the seismicity rate follows an acceleration (1992–1995) before a phase of deceleration (1995–2004). Rolandone et al. (2018) discusses this "typical of slow slip events" slip pattern where "slip shows a progressive acceleration before a phase of deceleration" similar to other subduction zones while investigating slow slip occurrences in central Equador.

We performed stochastic declustering (Zhuang, 2006; Zhuang et al., 2002, 2004) on the NEIC catalog (1974–2018) in the Cook Inlet region to remove cascading aftershocks and verified that the resulting catalog is consistent with a Poisson process at 95% confidence level, provided in this paper as supporting information. We found a mean $M \geq 3.0$ rate of 2.4/30 days before Slow Slip Event 1, which then increased to 5.3/30 days during Slow Slip Event 1, and then reduced slightly to 4.8/30 days during Slow Slip Event 2. These rate changes

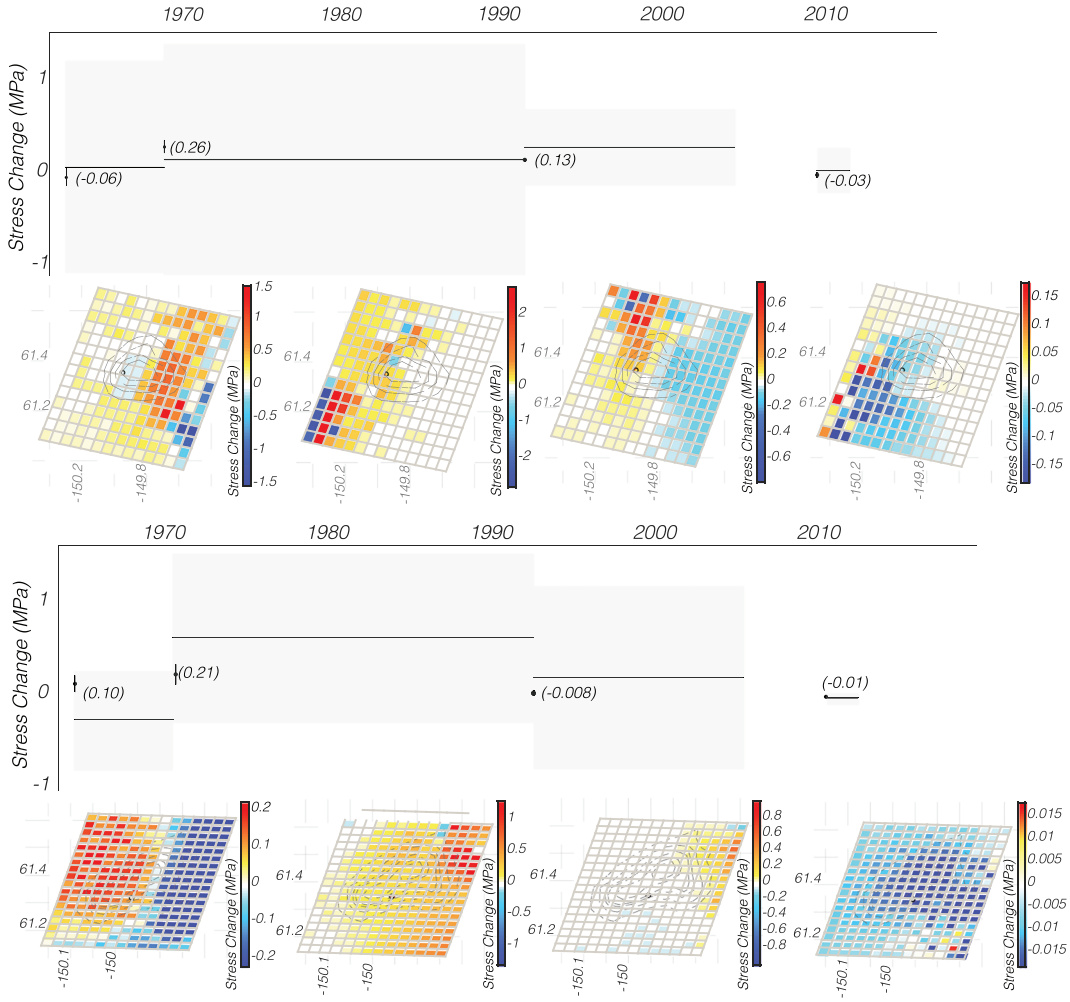

Figure 2. Stress history of the Anchorage 2018 rupture plane. We show (left to right) the stress changes resulting from the 1964 coseismic and postseismic, slow slip sources, Slow Slip Event 1: 1992.0–2004 (~*M*7.8), Slow Slip Event 2: 2009.85–2011.81 (~*M*7.2). The top and bottom panels are based on the USGS-NEIC and Liu et al. (2019) solution for the 2018 Anchorage event, respectively. For illustration purposes we show the coseismic values ending in 1970 and the postseismic until the estimated beginning of the slow slip events, although depending on the total afterslip value, important afterslip (>20 cm) may have occurred for more than 30 years after the 1964 earthquake (Suito & Freymueller, 2009). The horizontal black line represents the average value of stress changes on the fault plane for apparent friction coefficients $0 \leq \mu^{'} \leq 0.8$ with uncertainties shown in the shaded gray color area, the point value (in parenthesis) with error bars representing friction coefficients $0 \leq \mu' \leq 0.8$ at the start of each period corresponds to the stress at the hypocenter of the USGS-NEIC solution in (a) and of the Liu et al. (2019) solution in (b). Dashed lines on the fault plane (lower panel) represent the slip patch of each source model with values ranging between 0.2 and −1.8 m with $ds = 0.2$ m. Note the different saturation values for the graphic representation of stress changes among different sources.

are significant according to the Z statistic of Habermann (1981) and the β statistic of Matthews and Reasenberg (1988) at 95% confidence level, provided as supporting information.

The observed seismicity rate change pattern and the poor fit during Slow Slip Event 1 of the ETAS model (rate increase without a mainshock) provides evidence for the role of slow slip events in triggering deeper shallow depth seismicity. Following the end of Slow Slip Event 1, we observe that the average seismicity as described by our smoothed within 6-month windows seismicity (Figure 3, in black dashed) does not return to the pre–slow slip event level, but remains higher. The relatively short duration of Slow Slip Event 2 makes it difficult to assess its influence on seismicity rates, though we observe an increase in the average monthly rate (dashed black) in middle to late 2010 that the ETAS model cannot fit.

We have also considered stress change effects on the 2018 Anchorage earthquake from 15 $M \geq 5$ post-1990 events. These shocks occurred within ~50 km of the Anchorage epicenter and are within, or very close to, the

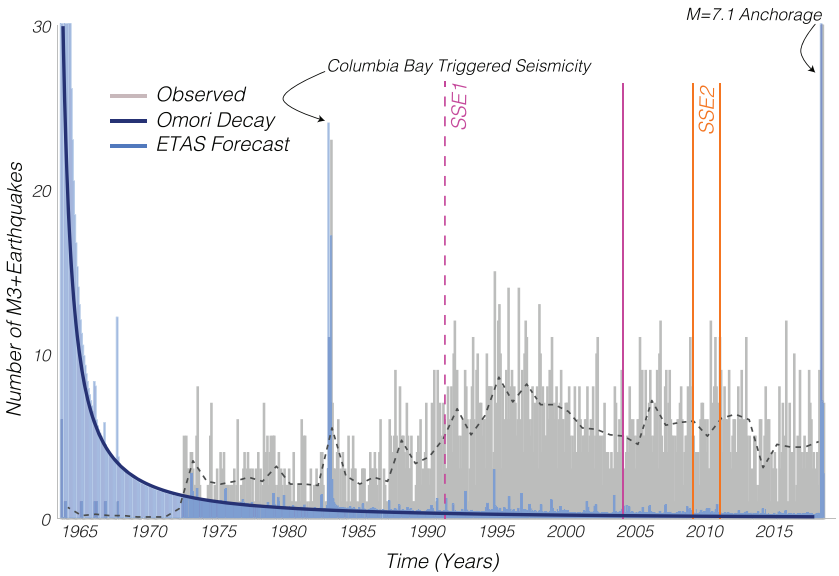

Figure 3. Post-1964 seismicity in the Cook Inlet region. The number of observed $M \geq 3$ earthquakes (gray) overlay by the expected number of events estimated by an ETAS model (light blue) within monthly intervals. The post-1964 triggered seismicity decay (dark blue) and the smoothed seismicity within 6-month windows (black *dashed*) is shown. Vertical lines mark the slow slip event durations; the start of Slow Slip Event 1 is represented by a dashed line since it coincides with the beginning of the network, as commented by Li et al. (2016). Note the seismicity pattern during the long Slow Slip Event 1 between 1992 and 2004.8 presents an increasing-decreasing section following the temporal slip distribution of slow slip events in other subduction zones; at the same time period the statistical ETAS model based solely on earthquake-to-earthquake interactions fails to describe the increasing seismicity.

slow slip event locations. We have considered both nodal planes from focal mechanisms and an average friction coefficient of $\mu' = 0.4$. The average maximum stress load from these events is miniscule, reaching 0.88 kPa, with maximum calculated stress change at 1.397 kPa from the 1991 *M*5.3, and 1.302 kPa from the 1997 *M*5.0 events. These stress change values fall well below the observed 0.01 MPa threshold for static triggering (Hardebeck et al., 1998; Harris & Simpson, 1992).

3. Slow Slip Event Stress Effects on the Megathrust

We investigate the influence of Coulomb failure stress change from past earthquake sources on the first slow slip event location. The recent mechanism proposed by Takagi et al. (2019) suggests that stress shadows of seismic asperities lead to an increased slip deficit that is more prominent updip, which causes steady creep or produces transient slow slip events but does not cause long-lasting slow slip events downdip of the seismic asperity. In the case of Alaska, we find that 0.80 and 0.92 of the total long-lasting Slow Slip Event 1 locations (alternatively stated 80%, 92%) are located within the 1964 Great Alaska earthquake stress shadow of the coseismic and postseismic slip distributions, respectively. The long-lasting Slow Slip Event 1 occurs on the subducting plane further downdip of the 1964 coseismic slip distributions, but within the upper limit of the 1964 afterslip at 30 km depth (Suito & Freymueller, 2009). However, as discussed in Rousset (2019), the variation of slip amplitudes in the Cook Inlet region remains quite poorly resolved, making conclusive results difficult.

We conclude that Slow Slip Event 1 promoted the occurrence of Slow Slip Event 2 in the period 2010–2012 because 62% of the Slow Slip Event 2 slip distribution was under positive stress change with a maximum of 0.23 MPa. We show calculated static stress changes from the cumulative slip distributions of Slow Slip Event 1 and Slow Slip Event 2 on the 3-D representation of the SLAB2.0 (Hayes, 2018) subduction interface (Figure S3). Following Slow Slip Event 1, we calculate an extended stress increased corridor beneath Anchorage at depths ranging between 20 and 60 km. The effects of Slow Slip Event 2 are spatially limited due to its smaller moment release with stress increase primarily NE of the 2018 Anchorage earthquake epicenter (Figure S3).

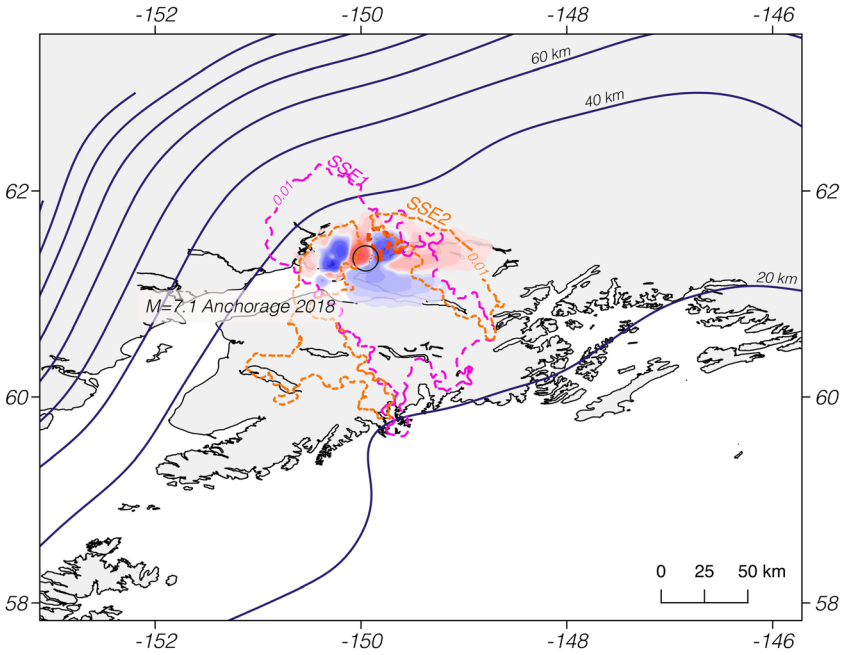

Figure 4. Coseismic stress changes on the megathrust. Colors describe the coseismic stress estimates following the *M*7.1 2018 Anchorage earthquake using the USGS-NEIC source model, the dashed red line denotes the positive stress locations using Liu et al. (2019) where the dashed magenta and orange lines encircle the positive stress locations that exceed 0.01 MPa using the cumulative slip of the Slow Slip Event 1 and Slow Slip Event 2, respectively.

Given the fact that slow slip events respond to small stress changes (as small as 0.015 MPa; Rubinstein et al., 2008), we consider the stress effects from the Anchorage earthquake on the slow slip event locations (Figure S3). We find that 74% of Slow Slip Event 1 locations are under positive stress change with a maximum Coulomb stress increase of 0.059 MPa (USGS-NEIC source model), and 21% of Slow Slip Event 1 locations are under positive stress change with a maximum Coulomb stress increase of 0.23 MPa (Liu et al., 2019, source model).

In Figure 4, we show the spatial distribution of coseismic stress changes on the subduction interface after the *M*7.1 2018 Anchorage earthquake considering both source models. The shallow USGS-NEIC source model supports a more extended spatial increase zone around Anchorage farther east and updip (0.01–0.02 MPa), whereas Liu et al. (2019) results in stress increase estimates immediately to the east of the epicenter (0.014–0.4 MPa).

We find that the positive (loading) effects of the slow slip events on the megathrust (Figure 4; in dashed orange, magenta lines) are more spatially extended when compared with the 2018 Anchorage stress changes. The slow slip events promoted slip on the megathrust at locations ranging from 20–60 km depth (Slow Slip Event 1; magenta line) and over 200 km along strike (Slow Slip Event 2; orange line) crossing between the locked and conditionally stable region, where both slow slip and seismic slip can occur. Considering the fact that the reoccurrence pattern of slow slip events is not well defined in Southcentral Alaska, it is difficult to anticipate whether the 2018 Anchorage event will shorten their recurrence interval. Dense monitoring from geodetic networks is required near Anchorage in order to determine with enhanced spatial resolution the onset of the next slow slip event.

4. Conclusions

We find that the 2018 *M*7.1 Anchorage normal intraslab earthquake is consistent with potentially being triggered by a combination of postseismic slip after the 1964 Great Alaska earthquake as well as by one to two slow slip episodes on the megathrust. The primary potential triggering sources were the slow-slip events that occurred between 1995 and 2004 that released a moment equivalent to a *M*7.8 earthquake. We demonstrate that the increase of low magnitude ($M \geq 3.0$) deeper shallow depth seismicity (20–60 km) in the Cook Inlet

region during the period between 1995 and 2004 is attributed to the slow slip event. This is evident because the rate increase within that period cannot be fit to standard ETAS models, the declustered catalog is consistent with a Poisson process, and the rate changes are statistically significant according to two methods.

Our analysis regarding the interplay between large earthquakes and slow slip events in Southcentral Alaska comes after the normal intraslab *M*7.1 2017 Puebla earthquake in Mexico that was likely triggered by extended delayed afterslip (*M*7.8) (Graham et al., 2014) along the subhorizontal subduction plane following the *M*7.5 2012 Oaxaca event (Segou & Parsons, 2018). A modulation of seismicity from slow slip events is identified in the Cascades region at the downdip edge of the megathrust (h = 40–60 km) (Vidale et al., 2011), but most commonly these responses are associated with shallow slow slip events for example in the Boso Pensinsula (Ozawa et al., 2003) and Hikurangi subduction zones (Delahaye et al., 2009). The above suggests that for short-term seismic hazard, incorporation of slow slip events or other aseismic phenomena is likely to play an important role in identifying high hazard locations for normal and thrust intraslab events that occur near the unstable, or conditionally stable, section of the subduction zone. Dense geodetic networks in the offshore and onshore region in Cook Inlet are required to improve the spatial and temporal resolution of the aseismic phenomena to allowing them to be incorporated into time-dependent seismic hazard assessment. In Southcentral Alaska the long-lasting slow slip events occur within the stress shadow of the 1964 earthquake and postseismic source. Although these slow slip events are found farther downdip of the 1964 coseismic slip distributions, they are within the upper limit of the 1964 afterslip slip region. The onset of slow slip events in the early 1990s may be related to 1964 postseismic effects, but assessing whether or not this is true would require geodetic data prior to the early 1990s, which does not exist.

Following the 2018 Anchorage earthquake, megathrust locations farther east and updip of the epicenter that are close to the shallow limit of the pre-earthquake slow slip event locations are positively loaded (0.01–0.4 MPa). At the same time the spatial distribution of past slow slip event related stress effects on the megathrust are far more extended. It remains to be seen the next few years whether the estimated stress effects of the 2018 Anchorage earthquake will modulate any future slow slip event locations farther east and updip of the hypocenter and/or will control the long-term deeper shallow depth seismicity rates in the region.

Acknowledgments
The authors have equally contributed the analysis and preparation of the manuscript. The authors would like to thank Natalia Ruppert from the Alaska Earthquake Center for providing the focal mechanism data for the post-1990 earthquakes in the region. All data used in the analysis of the Anchorage 2018 earthquake are available through the USGS event webpage (https://earthquake.usgs.gov/earthquakes/eventpage/ak20419010/executive). The ANSS earthquake catalog was also available through the USGS webpage (https://earthquake.usgs.gov/earthquakes/). We would like to thank the Editor, Jeroen Ritsema, and two anonymous reviewers for their constructive comments.

References

Alberto, Y., Kyokawa, H., Otsubo, M., Kiuota, T., & Towhata, I. (2018). Reconnaissanceof the 2017 Puebla, mexico earthquake. *Soils and Foundations*, *58*(5), 1073–1092.

Bilek, S. L., & Lay, T. (2018). Subduction zone megathrust earthquakes. *Geospheres*, *14*. https://doi.org/10.1130/GES01608.1

Choy, G., & Kirby, S. (2004). Apparent stress, fault maturity and seismic hazard for normal-fault earthquakes at subduction zones. *Geophysical Journal International*, *159*(3), 991–1012.

Delahaye, E. J., Townend, J., Reyners, M. E., & Rogers, G. (2009). Microseismicity but no tremor accompanying slow slip in the Hikurangi subduction zone, New Zealand. *Earth and Planetary Science Letters*, *277*, 21–28. https://doi.org/10.1016/j.epsl.2008.09.038

DeMets, C., Gordon, R. G., & Argus, D. F. (2010). Geologically current plate motions. *Geophysical Journal International*, *181*, 1–80.

Dmowska, R., & Lovison, L. C. (1988). Intermediate-term seismic precursors for some coupled subduction zones. *PAGEOPH*, *126*(2-4), 643–664. https://doi.org/10.1007/BF00879013

Eberhart-Phillips, D., Christensen, D. H., Brocher, T. M., Hansen, R., Ruppert, N. A., Haeussler, P. J., & Abers, G. A. (2006). Imaging the transition from Aleutian subduction to Yakutat collision in central Alaska, with local earthquakes and active source data. *Journal of Geophysical Research*, *111*, B11303. https://doi.org/10.1029/2005JB004240

Graham, S. E., DeMets, C., Cabral-Cano, E., Kostoglodov, V., Walperdorf, A., Cotte, N., et al. (2014). GPS constraints on the 2011/12 Oaxaca slow slip event that preceded the 20 March 2012 Ometepec earthquake, southern Mexico. *Geophysical Journal International*, *197*(3), 1593–1607. https://doi.org/10.1093/gji/ggu019

Habermann, R. E. (1981). Precursory seismicity patterns: Stalking the mature seismic gap. In D. W. Simpson, & P. G. Richards (Eds.), *Earthquake prediction—An international review*, (Vol. 11, pp. 29–42). Washington, D. C: American Geophysical Union.

Hardebeck, J. L., Nazareth, J. J., & Hauksson, E. (1998). The static stress change triggering model: Constraints from two southern California earthquake sequences. *Journal of Geophysical Research*, *103*, 24,427–24,437.

Harris, R. A. (1998). Introduction to special section: Stress triggers, stress shadows, and implications for seismic hazard. *Journal of Geophysical Research*, *103*, 24,347–24,358.

Harris, R. A., & Simpson, R. W. (1992). Changes in static stress on southern California faults after the 1992 landers earthquake. *Nature*, *360*, 251–254.

Hayes, G. (2018). Slab2—A comprehensive subduction zone geometry model: U.S. Geological Survey data release. https://doi.org/10.5066/F7PV6JNV

Hill, D. P., & Prejean, S. G. (2015). Dynamic triggering. In G. Schubert (Ed.), *Treatise on geophysics*, (2nd ed.pp. 273–304). Oxford: Elsevier.

Ichinose, G., Somerville, P., Thio, H. K., Graves, R., & O'Connell, D. (2007). Rupture process of the 1964 Prince William Sound, Alaska, earthquake from the combined inversion of seismic, tsunami, and geodetic data. *Journal of Geophysical Research*, *112*, B07306. https://doi.org/10.1029/2006JB004728

Ito, Y., Hino, R., Kido, M., Fujimoto, H., Osada, Y., Inazu, D., et al. (2013). Episodic slow slip events in the Japan subduction zone before the 2011 Tohoku-Oki earthquake. *Tectonophysics*, *600*, 14–26. https://doi.org/10.1016/j.tecto.2012.08.022

Kano, M., Kato, A., & Obara, K. (2019). Episodic tremor and slip silently invades strongly locked megathrust in the Nankai Trough. *Scientific Reports*, *9*(1), 9270. https://doi.org/10.1038/s41598-019-45781-0

Kato, A., Obara, K., Igarashi, T., Tsuruoka, H., Nakagawa, S., & Hirata, N. (2012). Propagation of slow slip leading up to the 2011 M_W 9.0 Tohoku-Oki earthquake. *Science*, *335*(6069), 705–708. https://doi.org/10.1126/science.1215141

Kobayashi, A., & Tsuyuki, T. (2019). Long-term slow slip event detected beneath the Shima Peninsula, central Japan, from GNSS data. *Earth, Planets and Space*, *71*, 6.

Lay, T., Ye, L., Ammon, C. J., & Kanamori, H. (2017). Intraslab rupture triggering megathrust rupture coseismically in the 17 December 2016 Solomon Islands *Mw* 7.9 earthquake. *Geophysical Research Letters*, *44*, 1286–1292. https://doi.org/10.1002/2017GL072539

Li, S., Freymueller, J., & McCaffrey, R. (2016). Slow slip events and time-dependent variations in locking beneath Lower Cook Inlet of the Alaska-Aleutian subduction zone. *Journal of Geophysical Research: Solid Earth*, *121*, 1060–1079. https://doi.org/10.1002/2015JB012491

Lin, J., & Stein, R. S. (2004). Stress triggering in thrust and subduction earthquakes and stress interaction between the southern San Andreas and nearby thrust and strike-slip faults. *Journal of Geophysical Research*, *109*, B02303. https://doi.org/10.1029/2003JB002607

Liu, C., Lay, T., Xie, Z., & Xiong, X. (2019). Intraslab deformation in the 30 November 2018 Anchorage, Alaska, *MW* 7.1 earthquake. *Geophysical Research Letters*, *46*, 2449–2457. https://doi.org/10.1029/2019GL082041

Llenos, A. L., & McGuire, J. J. (2011). Detecting aseismic strain transients from seismicity data. *Journal of Geophysical Research*, *116*, B06305. https://doi.org/10.1029/2010JB007537

Matthews, M. V., & Reasenberg, P. A. (1988). Statistical methods for investigating quiescence and other temporal seismicity patterns. *Pageoph*, *126*, 357–372.

Maury, J., Ide, S., Cruz-Atienza, V. M., & Kostoglodov, V. (2018). Spatiotemporal variations in slow earthquakes along the Mexican subduction zone. *Journal of Geophysical Research: Solid Earth*, *123*, 1559–1575. https://doi.org/10.1002/2017JB014690

Mikumo, T., Yagi, Y., Singh, S. K., & Santoyo, M. (2002). Coseismic and postseismic stress changes in a subducting plate: Possible stress interactions between large interplate thrust and intraplate normal-faulting earthquakes. *Journal of Geophysical Research*, *107*(B1), 2023. https://doi.org/10.1029/2001JB000446

Ogata, Y. (1985). Statistical models for earthquake occurrences and residual analysis for point processes, Research Memorandum, No. 288, The Institute of Statistical Mathematics, Tokyo, http://www.ism.ac.jp/editsec/resmemo/resm-j/resm-2j.htm.

Ohta, Y., Freymueller, J. T., Hreinsdottir, S., & Suito, H. (2006). A large slow slip event and the depth of the seismogenic zone in the south central Alaska subduction zone. *Earth and Planetary Science Letters*, *247*, 108–116. https://doi.org/10.1016/j.epsl.2006.05.013

Okada, Y. (1992). Internal deformation due to shear and tensile faults in a half-space. *Bulletin of the Seismological Society of America*, *82*, 1018–1040.

Omori, F. (1894). On the aftershocks of earthquakes. *Journal of the College of Science, Imperial University of Tokyo*, *7*, 111–120.

Ozawa, S., Miyazaki, S., Hatanaka, Y., Imakiire, T., Kaizu, M., & Murakami, M. (2003). Characteristic silent earthquakes in the eastern part of the Boso peninsula, Central Japan. *Geophysical Research Letters*, *30*(6), 1230. https://doi.org/10.1029/2002GL016665

Parsons, T. (2002). Global Omori law decay of triggered earthquakes: Large aftershocks outside the classical aftershock zone. *Journal of Geophysical Research*, *107*(B9), 2199. https://doi.org/10.1029/2001JB000646

Randall, W. J., Grant, A. R. R., Witter, R. C., Allstadt, K. E., Thompson, E. M., & Bender, A. M. (2019). Ground failure from the Anchorage, Alaska, earthquake of 30 November 2018. *Seismological Research Letters*, *91*(1), 19–32. https://doi.org/10.1785/0220190187

Rice, J. R. (1992). Fault stress states, pore pressure distributions, and the weakness of the San Andreas Fault. In B. Evans, & T. Wong (Eds.), *Fault mechanics and transport properties of rocks; a festschrift in honor of W. F. Brace*, (pp. 475–503). San Diego, CA, USA: Academic Press.

Rolandone, F., Nocquet, J. M., Mothes, P. A., Jarrin, P., Vallée, M., Cubas, N., et al. (2018). Areas prone to slow slip events impede earthquake rupture propagation and promote afterslip. *Science Advances*, *4*(1), eaao6596. https://doi.org/10.1126/sciadv.aao6596

Rousset, B. (2019). Months-long subduction slow slip events avoid the stress shadows of seismic asperities. *Journal of Geophysical Research: Solid Earth*, *124*, 7227–7230. https://doi.org/10.1029/2019JB018037

Rousset, B., Fu, Y. & Burgmann, R. (2018). Characterization of slip pulses within the upper Cook Inlet 2008–2013 slow slip event in Alaska, American Geophysical Union, Fall Meeting 2018, abstract #T33F-0479.

Rubinstein, J. L., La Rocca, M., Vidale, E., Creager, K. C., & Wech, A. G. (2008). Tidal modulation of non-volcanic tremor. *Science*, *300*(5627), 1942–1943.

Ruiz, S., Metois, M., Fuenzalida, A., Ruiz, J., Leyton, F., Grandin, R., et al. (2014). Intense foreshock and slow slip event preceded the 2014 Iquique M_w 8.1 earthquake. *Science*, *345*(6201), 1165–1169. https://doi.org/10.1126/science.1256074

Ruppert, N. A., & West, M. E. (2019). The impact of USArray on earthquake monitoring in Alaska. *Seismological Research Letters*, *91*(2A), 601–610. https://doi.org/10.1785/0220190227

Ruppert, N. A., & Witter, R. (2019). Preface to the focus section on the 30th November 2018, *Mw* 7.1, Anchorage, Alaska Earthquake. *Seismological Research Letters*, *91*, 16–18. https://doi.org/10.1785/0220190344

Segou, M., & Parsons, T. (2018). Testing earthquake links in Mexico from the 1978 M7.6 Oaxaca to the 2017 M7.1 Puebla shock. *Geophysical Research Letters*, *45*, 708–714. https://doi.org/10.1002/2017GL076237

Segou, M., Parsons, T., & Ellsworth, W. (2013). Comparative evaluation of physics-based and statistical forecasts in Northern California. *Journal of Geophysical Research - Solid Earth*, *118*, 6219–6240. https://doi.org/10.1002/2013JB010313

Singh, S. K., Ordaz, M., Alcantara, L., Shapiro, N., Kostoglodov, V., Pacheco, J. F., et al. (2000). The Oaxaca earthquake of 30 September 1999 (*Mw*-7.5): A Normal-faulting event in the subducted Cocos plate. *Seismological Research Letters*, *71*(1), 67–78. https://doi.org/10.1785/gssrl.71.1.67

Suito, H., & Freymueller, J. T. (2009). A viscoelastic and afterslip postseismic deformation model for the 1964 Alaska earthquake. *Journal of Geophysical Research*, *114*, B11404. https://doi.org/10.1029/2008JB005954

Takagi, R., Uchida, N., & Obara, K. (2019). Along-strike variation and migration of long-term slow slip events in the western Nankai subduction zone, Japan. *Journal of Geophysical Research: Solid Earth*, *124*, 3853–3880. https://doi.org/10.1029/2018JB016738

Vidale, J. E., Hotovec, A. J., Ghosh, A., Creager, K. C., & Gomberg, J. (2011). Tiny intraplate earthquakes triggered by nearby episodic tremor and slip in Cascadia. *Geochemistry, Geophysics, Geosystems*, *12*, Q06005. https://doi.org/10.1029/2011GC003559

Voss, N., Dixon, T. H., Liu, Z., Malservisi, R., Protti, M., & Schwartz, S. (2018). Do slow slip events trigger large and great megathrust earthquakes? *Science Advance*, *4*, eaat8472.

Voss, N. K., Malservisi, R., Dixon, T. H., & Protti, M. (2017). Slow slip events in the early part of the earthquake cycle. *Journal of Geophysical Research: Solid Earth*, *122*, 6773–6786. https://doi.org/10.1002/2016JB013741

Wallace, L. M., Bartlow, N., Hamling, I., & Fry, B. (2014). Quake clamps down on slow slip. *Geophysical Research Letters*, *41*, 8840–8846. https://doi.org/10.1002/2014GL062367

Wei, M., McGuire, J. J., & Richardson, E. (2012). A slow slip event in the south central Alaska subduction zone and related seismicity anomaly. *Geophysical Research Letters*, *39*, L15309. https://doi.org/10.1029/2012GL052351

Zechar, J. D., Gerstenberger, M. C., & Rhoades, D. A. (2010). Likelihood based tests for evaluating space-rate-magnitude earthquake forecasts. *Bulletin of the Seismological Society of America*, *100*, 1184–1195. https://doi.org/10.1785/0120090192

Zhuang, J. (2006). Second-order residual analysis of spatiotemporal point processes and applications in model evaluation. *Journal of the Royal Statistical Society, Series B: Statistical Methodology*, *68*(4), 635–653. https://doi.org/10.1111/j.1467-9868.2006.00559.x

Zhuang, J., Ogata, Y., & Vere-Jones, D. (2002). Stochastic declustering of space-time earthquake occurrences. *Journal of the American Statistical Association*, *97*, 369–380.

Zhuang, J., Ogata, Y., & Vere-Jones, D. (2004). Analyzing earthquake clustering features by using stochastic reconstruction. *Journal of Geophysical Research*, *109*, B05301. https://doi.org/10.1029/2003JB002879

References From the Supporting Information

Cameron, A. C., & Trivedi, P. K. (1998). *Regression analysis of count data*, (p. 411). New York: Cambridge Press.

Gutierrez, R. G., Carter, S., & Drukker, D. M. (2001). On boundary-value likelihood-ratio tests. *Stata Technical Bulletin*, *60*, 15–18.

Hilbe, J. M. (2011). *Negative binomial regression*, (2nd ed.,p. 576). New York: Cambridge University Press.

Luen, B., & Stark, P. B. (2012). Poisson tests of declustered catalogues. *Geophysical Journal International*, *189*(1), 691–700. https://doi.org/10.1111/j.1365-246X.2012.05400.x

Ogata, Y. (1988). Statistical models for earthquake occurrences and residual analysis for point processes. *Journal of the American Statistical Association*, *83*, 9–27.

Ogata, Y. (1992). Detection of precursory relative quiescence before great earthquakes through a statistical model. *Journal of Geophysical Research*, *97*, 19,845–19,871.

Ogata, Y., & Zhuang, J. (2006). Space-time ETAS models and an improved extension. *Tectonophysics*, *413*, 13–23. https://doi.org/10.1016/j.tecto.2005.10.016

Wang, Q., Jackson, D. D., & Zhuang, J. (2010). Missing links in earthquake clustering models. *Geophysical Research Letters*, *37*, L21307. https://doi.org/10.1029/2010GL044858